Polar Biology (2024) 47:1575–1592
https://doi.org/10.1007/s00300-024-03306-0

RESEARCH

In-situ observations of gelatinous zooplankton aggregations in inshore and offshore Arctic waters

Dmitrii Pantiukhin[1,2] · Joan J. Soto-Angel[3] · Aino Hosia[3] · Henk-Jan Hoving[4] · Charlotte Havermans[1,2]

Received: 19 January 2024 / Accepted: 19 September 2024 / Published online: 4 November 2024

Abstract

Gelatinous zooplankton (GZ), play a crucial role in marine food webs, nutrient cycling, and carbon sequestration, however, quantifying their abundances remains challenging due to their delicate body structure, complex life cycles and variable population dynamics. Their tendency to form sporadic, large-scale aggregations further complicate the differentiation between true ecosystem alterations and stochastic variations in their abundance. In the Arctic Ocean, our understanding of GZ aggregations remains generally incomplete. Using *in-situ* observations from a towed pelagic camera system, we assessed the diversity and vertical distributions of GZ in fjord and offshore environments in northern Norway and the Svalbard archipelago. We found that Atlantic water masses harbored the highest GZ abundance, while intermediate waters showed the highest diversity. We documented dense aggregations of *Beroe* spp. in Van Mijenfjorden in Svalbard (observed during ascent of the camera system, not quantified in ind. m^{-3}) and *Bolinopsis infundibulum* in the open Barents Sea (> 2.67 ind. m^{-3} at 100 m). Other observed taxa included the hydrozoans *Aglantha digitale*, *Melicertum octocostatum, Solmundella bitentaculata,* Pandeidae sp. and Physonectae spp., the scyphozoan *Cyanea capillata* and the ctenophores *Mertensia ovum* and *Euplokamis* sp. By linking the vertical distribution and observations of local aggregations with physical and biotic factors, we described the potential drivers of the distributional patterns observed. Towed camera surveys contribute to accurate *in-situ* observations, thereby improving our understanding of GZ aggregations and distributions in the Arctic Ocean.

Keywords Ctenophore aggregations · Gelatinous zooplankton · Beroe · Bolinopsis · Underwater towed camera · Arctic Ocean

Introduction

Gelatinous zooplankton (GZ) are a polyphyletic group of marine animals that share traits of high water concentration in their bodies (often over 95% of wet weight, Lüskow et al. 2021) and an inherent fragility (Larson 1986). GZ includes taxa belonging to the phyla Cnidaria (scyphozoans, hydromedusae and siphonophores), Ctenophora and Chordata (appendicularians, doliolids, salps), which play an essential role in marine food webs, nutrient cycling, and carbon sequestration (Choy et al. 2017; Luo et al. 2020). GZ are often characterized by rapid growth, short generation times and high grazing or predation pressures, particularly when occurring in high numbers (Alldredge 1984). Most GZ groups have the ability to form large aggregations that are influenced by a complex of physical, behavioral, and reproductive factors (Dawson and Hamner 2009; Fernández-Alías et al. 2021). Large aggregations are broadly categorized into (i) physical aggregations, which are driven by hydrographic features such as gradients in physical factors near the pycno/thermo/halocline (e.g., Raskoff et al. 2005), or by surface, wind-driven features (e.g., Hamner & Schneider 1986) and seafloor characteristics (Graham et al. 2001), and (ii) blooms, which are associated with seasonal reproductive events (e.g., Arai 1992). Physical aggregations also

✉ Dmitrii Pantiukhin
dmitrii.pantiu@gmail.com

1 HYIG ARJEL, Benthic Ecology, Alfred Wegener Institute Helmholtz Centre for Polar and Marine Research, Bremerhaven, Germany

2 Marine Zoology, BreMarE, Bremen Marine Ecology, FB2, University of Bremen, Bremen, Germany

3 Department of Natural History, University Museum of Bergen, University of Bergen, Bergen, Norway

4 GEOMAR Helmholtz Centre for Ocean Research Kiel, Kiel, Germany

include the complexity of demographic changes, such as different distribution patterns of juveniles and adults in the water column (Batistić et al. 2004), and diurnal vertical migrations (Graham et al. 2001). What triggers GZ blooms and aggregations, and how they are organized in time and space, is to a large extent not well understood (Hamner and Dawson 2009).

Gelatinous zooplankton can be divided into holo- and meroplanktonic species, with the latter having a benthic polyp stage, controlling the release and development of small medusae and hence adding complexity to their bloom dynamics. GZ blooms, including those of Scyphozoa, Hydrozoa, and Ctenophora, are either initiated by the release of medusae by benthic polyps in Scyphozoa and Hydrozoa, or through reproductive peaks in holoplanktonic Cnidaria and Ctenophora, resulting in sequential seasonal peaks in abundance among species (Mills 2001). Members of the Class Scyphozoa are particularly notable for their blooming potential (Fernández-Alías et al. 2021), reaching densities of several thousand medusae per square meter (Hari Praved et al. 2021). GZ, such as Ctenophora, can also form dense aggregations. However, they are usually poorly documented due to their fragility and the associated challenges when applying traditional collection methods (Hosia et al. 2017). These traditional methods, such as net tows, do not always yield reliable datasets, particularly for estimating the abundance and biomass of more fragile GZ like ctenophores and appendicularians (e.g., Hosia et al. 2017; Long et al. 2020). These methods usually fragment or entirely destroy individuals of the more delicate species. Moreover, despite their efficiency of sampling large water volumes and biomasses over large areas, these sampling gear fail to detect local aggregations and fine-scale patchiness. In contrast to traditional methods, optical imaging techniques, such as cameras on remotely operated vehicles (Robison 2004), vertical profiling cameras (Picheral et al. 2022) and horizontally towed pelagic cameras, provide non-invasive, high-resolution observations (Hoving et al. 2019). These *in-situ* systems allow organisms to be recorded without damaging their structural integrity, avoiding the problems associated with fragmentation or destruction of gelatinous organisms. In addition, their application enhances our ability to determine distribution gradients with higher resolution and allows the detection of local aggregation patterns.

Recent studies have hypothesized an increase in the abundance of GZ worldwide (Brotz et al. 2012), a phenomenon often referred to as "ocean jellification" (Roux et al. 2013). However, substantial support for this hypothesis is lacking, largely due to the paucity of comprehensive spatio-temporal datasets (Condon et al. 2013). This is further complicated by the difficulty of distinguishing intra- and interannual population fluctuations from global, climate-change driven trends (Purcell 2005).

The Arctic Ocean is undergoing rapid ecological changes, and these changes are driven by temperatures that are rising four times faster than the global average and causing major sea-ice retreat (Fox-Kemper et al. 2021). Physical changes induce major oceanographic phenomena such as the influx of warmer, temperate waters into the Arctic Ocean, via both the Pacific and Atlantic gateways, referred to as 'pacification' and 'atlantification', respectively (Polyakov et al. 2020; Ingvaldsen et al. 2021). This warm water influx causes shifts in communities, where cold-water Arctic species are being replaced by their boreal counterparts, a process which is increasingly reported for the Atlantic sector of the Arctic Ocean (Polyakov et al. 2020; Ingvaldsen et al. 2021). Despite the general lack of studies on distributional patterns of GZ in the region, recent studies (Mańko et al. 2020; Pantiukhin et al. 2023) projected that several species with an affinity for Atlantic waters, such as the hydrozoan *Aglantha digitale*, will become increasingly abundant with further atlantification, while some species with cold-water affinity, such as *Sminthea arctica*, will significantly decrease in numbers (Pantiukhin et al. 2023, 2024). Several key GZ species, such as the scyphozoan *Cyanea capillata* and *Periphylla periphylla*, ctenophores such as *Beroe* spp., and appendicularians including *Fritillaria borealis*, were predicted to expand their ranges with future climate-change projections (Pantiukhin et al. 2024).

Recent studies have characterized spatial distributions of GZ in the Arctic using depth-stratified plankton nets (Mańko et al. 2020), under-ice trawls (David et al. 2015), or optical surveys (Remotely Operated Vehicles in Raskoff et al. 2005, 2010; PELAGIOS in Pantiukhin et al. 2023). Nonetheless, the study of regional or local aggregation dynamics of GZ in the Arctic, especially in fjord and shelf systems of the European Arctic, remains poorly documented. The aforementioned studies could link species distributions with the complex and multi-origin water layers typical of the Arctic Ocean (Raskoff et al. 2005; Purcell et al. 2010). Indeed, the Arctic Ocean is characterized by strong near-surface discontinuities in temperature and salinity. The interaction of warm, salty Atlantic waters and cold, fresher Polar waters, as well as meltwater from sea-ice, can generate sharp submesoscale fronts (von Appen et al. 2018).

The environmental characteristics of Arctic fjord systems are characterized by the relative influence of the different water masses, as well as by sea-ice processes and marine-terminating glaciers more inwards into the fjord (Cottier et al. 2010). In Svalbard, the Kongsfjorden and Krossfjorden fjords are connected by a common mouth, through which they experience a strong exchange with the warm West Spitsbergen Current (Svendsen et al. 2002). Both fjords are strongly influenced by tidewater glaciers (seven glaciers in Kongsfjorden, only one in Krossfjorden). To the south lies Van Mijenfjorden, which is less glaciated and has the

characteristics of a semi-enclosed fjord (Skarðhamar and Svendsen 2010). Due to its narrow mouth and the presence of the island of Akseløya, the influence of the West Spitsbergen Current is reduced compared to the Kongsfjorden–Krossfjorden system, while the importance of the local hydrography (e.g., landfast ice and discharging rivers) is known to be more pronounced (Skarðhamar and Svendsen 2010). Hornsund is the southernmost fjord of Svalbard. Only 34 km long, it has a wide mouth that allows free entry of both cold surface Arctic water masses and the warm West Spitsbergen Current (Błaszczyk et al. 2013). The hydrography is also complicated by the presence of strong tidewater glacier discharge from fourteen glaciers, resulting in strong stratification of the fjord (Swerpel 1985). The Barents Sea region is influenced by significant amounts of Atlantic water, which cools and mixes with other water masses in the region (Jakobsen and Ozhigin 2011). Finally, Porsangerfjorden, the largest fjord in northern Norway, is divided into an outer and inner basin, where the outer basin is more influenced by the Norwegian coastal current, while the inner basin is characterized by cold Arctic waters of local origin (Svendsen 1991; Wassmann et al. 1996).

With regard to the association of zooplankton with different water masses, it has been hypothesized that Atlantic water masses bring more diverse and abundant communities to the Arctic (Hop et al. 2019). Conversely, other studies recorded higher abundances of GZ in Atlantic water masses, while Arctic waters harbored a higher species richness (Mańko et al. 2020; Pantiukhin et al. 2023).

The main goal of this study is to describe and characterize GZ aggregations in Arctic waters. To do this, we have conducted optical surveys in three different marine environments: fjord systems of the high Arctic Svalbard archipelago, a fjord system in northern Norway mainland, and the open waters of the Barents Sea shelf (Fig. 1). Specifically, to investigate the occurrence of aggregations and small-scale vertical distributions of GZ in the Arctic Ocean, their link to different water masses and potential other environmental factors driving them, we conducted optical surveys at several localities along a poleward gradient, including the fjords of Svalbard, the open waters of the Barents Sea and the largest fjord of northern Norway, i.e., Porsangerfjorden, all of which are under differing influence of Atlantic waters. By carrying out depth-layered transects with a towed video camera system, we aimed to elucidate the spatial distribution of GZ in the water column and to quantify their local populations. Using these data, we estimated the abundance of GZ at specific depths and interpreted the findings in the context of the abiotic and biotic conditions at each station. This study provides a solid foundation for understanding the GZ aggregations and their spatial dynamics in the Arctic region. Additionally, our work contributes to establishing further baselines of local spatial patterns of GZ in different Arctic marine

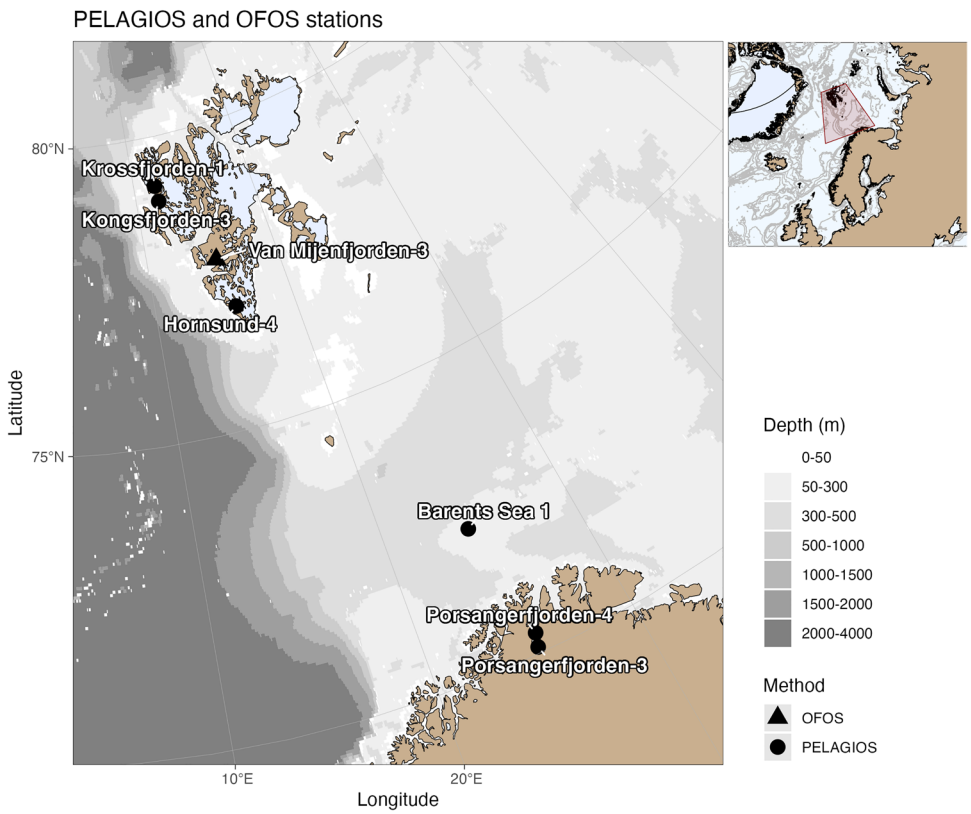

Fig. 1 Map displaying the geographic locations of the different deployments of the Pelagic In-situ Observation System (PELAGIOS) and the Ocean Floor Observation System (OFOS) along a poleward gradient from northern Norway to Svalbard

environments, which is crucial for improving the detection of species shifts with continued atlantification.

Methods

Study area and deployments during the R/V Heincke expedition HE605

During the HE605 expedition "RISING" with the research vessel R/V Heincke (Alfred Wegener Institute 2017) in August 2022 over 15 days (Havermans 2023), we deployed the Pelagic In Situ Observing System (PELAGIOS; Hoving et al. 2019) and the Ocean Floor Observation System (OFOS; Alfred Wegener Institute 2017) to observe Arctic epi- and mesopelagic ecosystems along a poleward gradient (Fig. 1, Table 1). The surveys were conducted in four fjords in the western Svalbard archipelago (Krossfjorden, Kongsfjorden, Hornsund, and Van Mijenfjorden), one station in the Barents Sea shelf zone, and one fjord in northern Norway (Porsangerfjorden). These optical transects were preceded by the physical characterisation of the water masses using a CTD rosette (see below).

The Pelagic In-situ Observation System (PELAGIOS) is a high-definition video camera system that records at 50 frames per second. It was towed horizontally from the side of the research vessel at a speed of approximately 1 knot, covering different depth layers within the water column. The resulting horizontal profiles were carried out in depths from 3 to 300 m, in order to cover a representative range of GZ habitats and to cover the entire water column (Fig. 2). Due to the design of the PELAGIOS system, we only used data from horizontal transects for quantitative taxa estimation, while for the ascent and descent phases, we only reported

Table 1 Details on the analyzed PELAGIOS and OFOS surveys of the HE605 expedition

Event label	Optional label	Method/device	Date	Time (UTC)	Latitude start	Longitude start	Latitude end	Longitude end
HE605_1-5	Krossfjorden-1	PELAGIOS	2022-08-15	10:55:50	79° 12,230' N	011° 48,984′ E	79° 10,728′ N	011° 47,350′ E
HE605_5-5	Kongsfjorden-3	PELAGIOS	2022-08-16	9:45:05	78° 56,775′ N	011° 54,472′ E	78° 56,923′ N	011° 56,453′ E
HE605_12-5	Van Mijenfjorden-3	OFOS	2022-08-18	11:39:00	77° 48,376′ N	015° 19,359′ E	77° 47,543′ N	015° 19,499′ E
HE605_16-1	Hornsund-4	PELAGIOS	2022-08-19	21:10:50	76° 59,266′ N	015° 49,480′ E	76° 58,474′ N	015° 46,889′ E
HE605_18-5	Barents Sea-1	PELAGIOS	2022-08-21	8:11:26	72° 17,892′ N	024° 27,466′ E	72° 19,016′ N	024° 28,586′ E
HE605_23-13	Porsangerfjorden-3	PELAGIOS	2022-08-24	10:12:18	70° 06,501′ N	025° 09,047′ E	70° 07,411′ N	025° 10,683′ E
HE605_24-14	Porsangerfjorden-4	PELAGIOS	2022-08-25	10:35:31	70° 19,865′ N	025° 19,635′ E	70° 21,173′ N	025° 20,203′ E

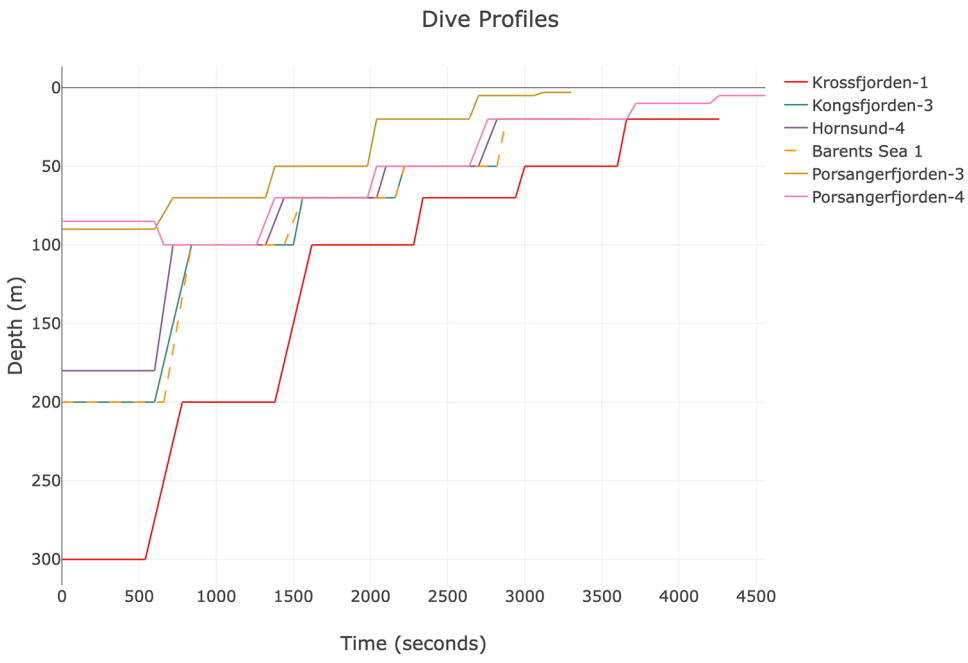

Fig. 2 Graphical representation of the dive transects of the PELAGIOS video system

counts of encountered individuals for each taxa. In total, we performed 33 unique horizontal transects at the six studied stations, representing ~ 5.6 h of videos. The majority of these transects had a duration of 10 min (Fig. 2). Out of the multiple Ocean Floor Observation System (OFOS) stations during the HE605 expedition, we have only included one survey, as the major focus of these transects are the fauna residing on the seafloor. During the survey in the Van Mijenfjorden station we observed a conspicuously high number of ctenophores during the ascent of the OFOS survey, hence, this dive has been further analyzed.

Biological data

The optical data from the cruise were analyzed in the marine image annotation tool BIIGLE 2.0 (biigle.de; Langenkämper et al. 2020). First, the video files were converted from MTS video format to MPEG-4/H.264 using the ffmpeg software (https://ffmpeg.org). The data were then manually annotated using 'point annotation' in BIIGLE 2.0. The resulting count data from the PELAGIOS transects were converted to individuals per 1000 m^3 using the formula described in Hoving et al. (2019). Each 10-min video tow captured approximately 69.6 m^3 of water, based on an average recorded volume of 0.116 m^3 per second at a towing speed of approximately 1 knot. Data from the ascending and descending transects could not be converted to the same format due to their biased estimates, thus they are presented as normal counts in Table S1. OFOS data are also presented as counts for every 10 m of ascent. The majority of gelatinous taxa encountered were annotated to species-level (Fig. 3); annotations of *Beroe* were only to genus level (listed as *Beroe* spp.) since this is a poorly resolved species complex (Bayha et al. 2004; Johansson et al. 2018; Shiganova and Abyzova 2022) and molecular analyses have shown that diagnostic characters of *Beroe* in Arctic waters are currently insufficiently delimited (Jucker and Havermans 2022).

In terms of taxonomic delineation, *Euplokamis* sp. was identified by the conspicuous arrangement of typically coiled tentilla resembling droplets, *Pleurobrachia* sp. was categorized based on its "egg-shaped" body and numerous tentilla when visible. Broad categories such as Ctenophora spp. and Cydippida spp. were used for lower quality images and include several morphological types. In the case of *Beroe* spp., its morphotype was aligned with *Beroe cucumis*, but due to the aforementioned problems with current species delimitations (Jucker and Havermans 2022), it is placed at the level of *Beroe* spp. The ctenophore *M. ovum* was identified based on their flattened appearance, pointed oral region and contrasting keels in the aboral region, followed by tentacles when extended. The lobate ctenophore *B. infundibulum* was recognized by the presence of large lobes, rounded in lateral view and contrasting with the flattened aboral region, or their elongated general shape in frontal view. The hydrozoan *M. octocostatum* was determined by the observation of 8 clear bands representing the gonads in the radial canals.

Environmental data

During the HE605 expedition, environmental data for temperature (°C), salinity (PSU), oxygen concentration (ml l^{-1}), and fluorescencE (mg m^{-3}) were collected at each PELAGIOS and OFOS station using the CTD system (SBE911plus). The CTD sensors included SBE3plus

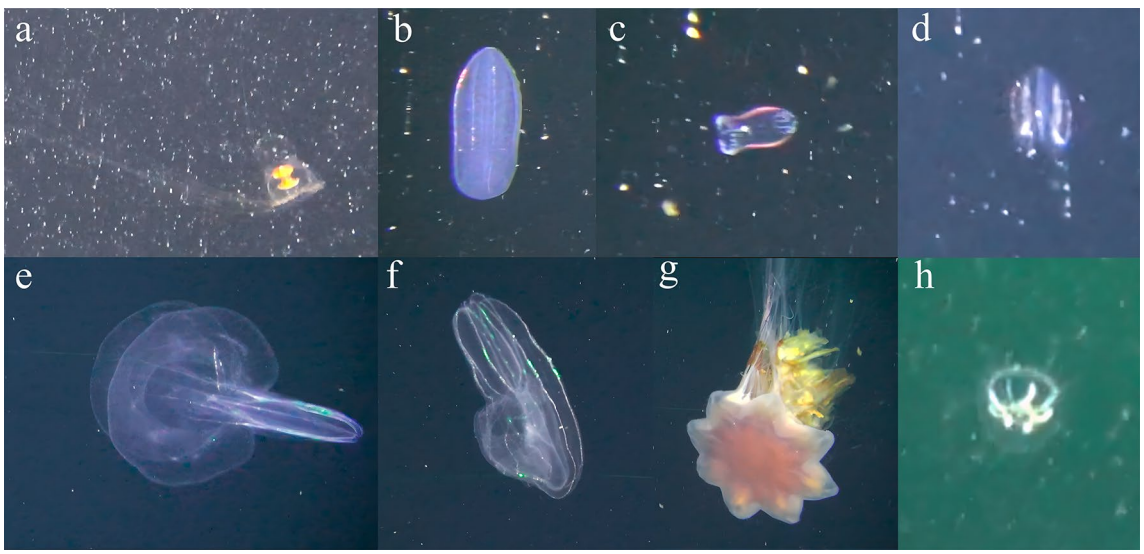

Fig. 3 Examples of gelatinous zooplankton detected by the PELAGIOS video system. **a** Pandeidae sp.; **b** *Beroe* sp.; **c** *Aglantha digitale*; **d** *Mertensia ovum*; **e, f** *Bolinopsis infundibulum*; **g** *Cyanea capillata*; **h** *Melicertum octocostatum*

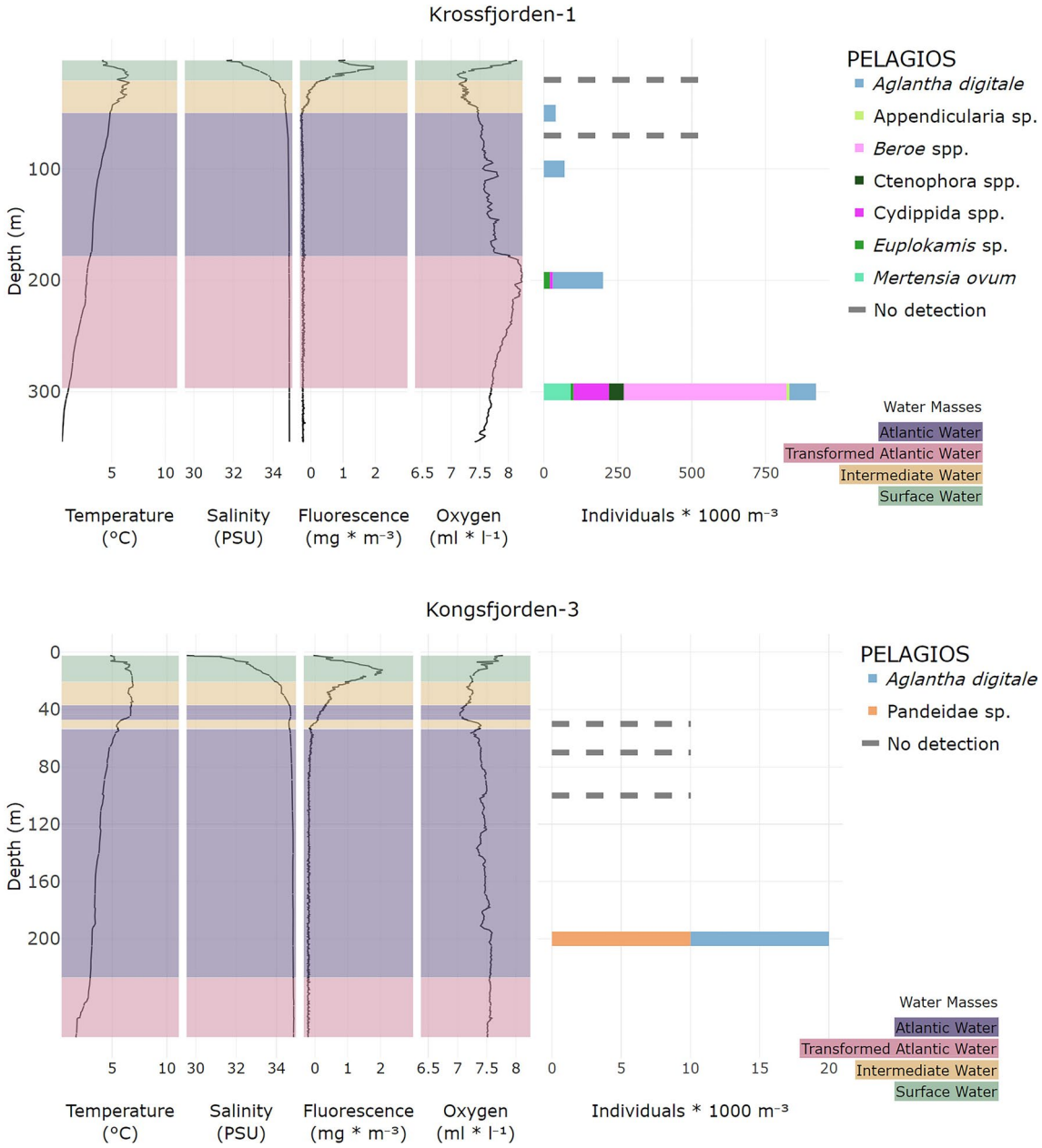

Fig. 4 Depth distribution of gelatinous zooplankton by station at different depths with corresponding CTD data. Data from the PELAGIOS video system are presented in individuals per cubic meter, while OFOS data are presented in counts only. Water mass classification is adapted from Cottier et al. (2005)

for temperature, SBE4c for conductivity, an oxygen sensor (SBE43), a transmissometer (WetLabs CStar), a fluorometer (WetLabs, EcoFl) for chlorophyll-a concentration and an altimeter (Benthos, PSA 900D). In Porsangerfjorden, PELAGIOS was deployed deeper than the CTD rosette due to the difficulties associated with the underwater topography. Similarly, the CTD did not cover the full depth profile compared to the OFOS dive, also due to the same reason. The oceanographic data for each PELAGIOS station was derived from the nearest corresponding CTD station. Further the water masses were classified according to Cottier et al. (2005), including Atlantic Water (AW, $T > 3$ °C, $S > 34.65$), Arctic Water (ArW, $T -1.5$ to 1.0 °C, S 34.30–34.80), Winter Cooled Water (WCW, $T < -0.5$ °C, S 34.40–35.00), Local Water (LW, $T -0.5$ to 1.0 °C, S 34.30–34.85), Surface Water (SW, $T > 1.0$ °C, $S < 34.00$), Transformed Atlantic Water (TAW, T 1.0–3.0 °C, $S > 34.65$), and Intermediate Water (IW, $T > 1.0$ °C, S 34.00–34.65; Table S1; Fig. 4).

To further interpret the dynamics of GZ aggregations, we also collected satellite data on the concentration of

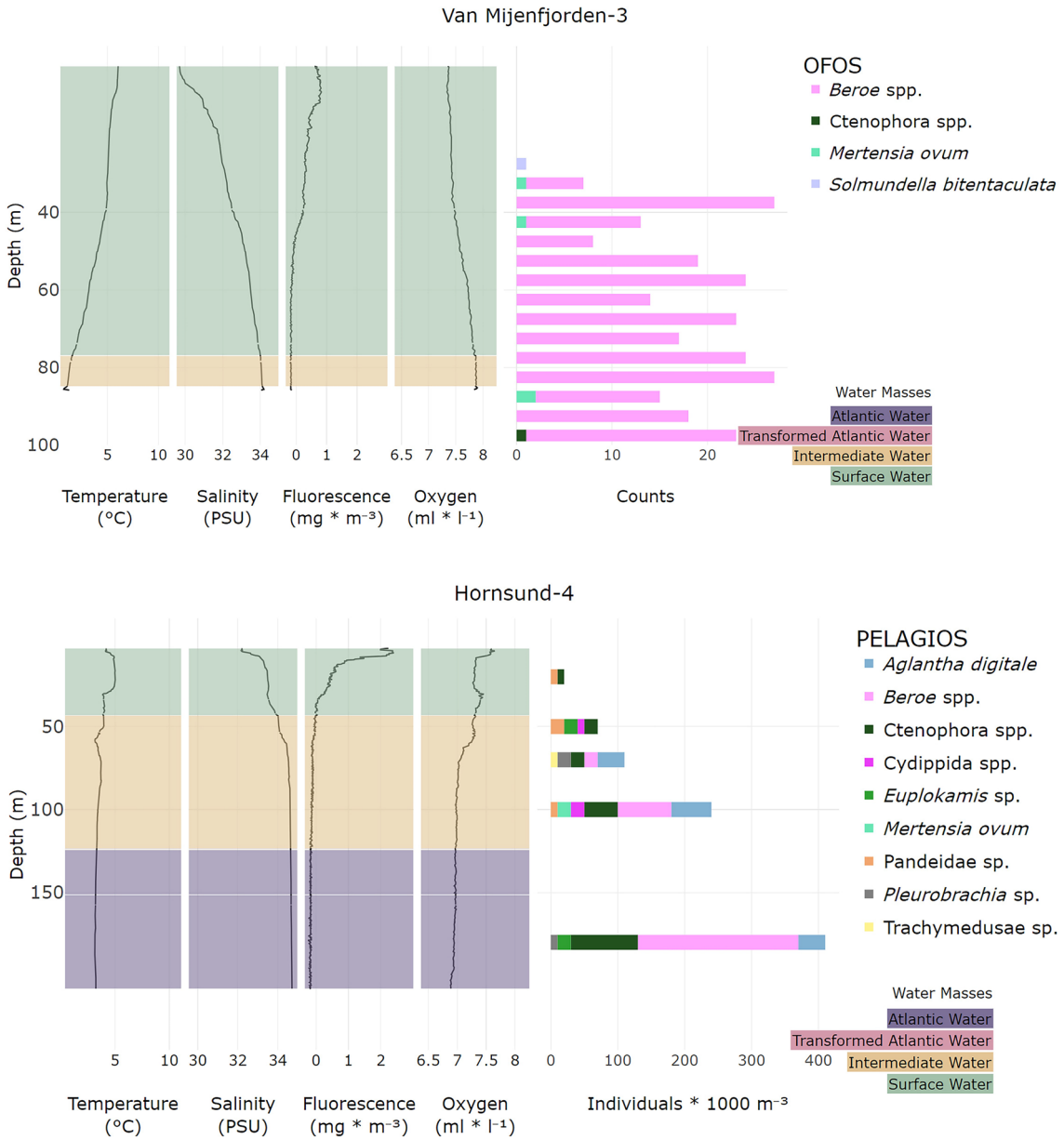

Fig. 4 (continued)

phytoplankton in the surface waters in the upper 25 m (mg m^{-3}), as well as a re-analysis of the potential temperature (°C) and salinity (PSU). The chlorophyll concentration data were obtained from the AQUA MODIS satellite and were retrieved from oceancolor.gsfc.nasa.gov (OCI algorithm). We examined chlorophyll concentration data from 8 days prior to the sampling event (13.08–20.08; Fig. 5) to track the dynamics of potential phytoplankton blooms at the sampling sites. The data were extracted from data.marine.copernicus.eu and represent daily projections of these values from 2018 to mid-2023 (Sakov et al. 2012; Melsom et al. 2012).

Statistical analysis

To assess the relationships between GZ communities and environmental factors, we employed a series of statistical analyses using R (version 4.3.2; R Core Team 2023). Species richness was calculated using the specnumber function from the vegan package (version 2.5-7; Oksanen et al. 2024).

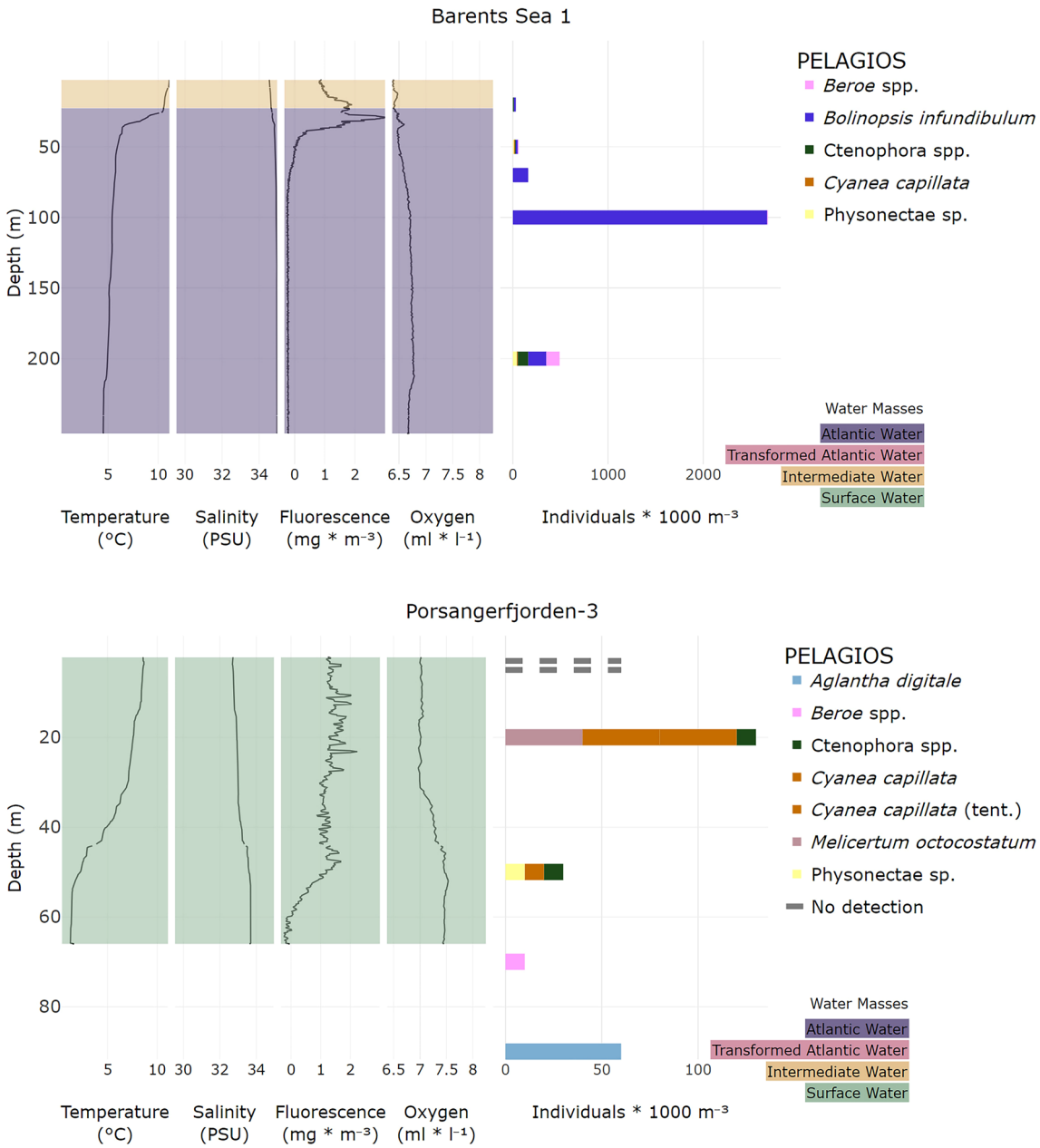

Fig. 4 (continued)

We conducted one-way ANOVAs followed by Tukey's HSD post-hoc tests to examine differences in species richness and total abundance across water masses. Principal component analysis (PCA) was performed on the Hellinger-transformed species abundance data to visualize community composition patterns. To test the effects of environmental variables on community structure, we used Permutational Multivariate Analysis of Variance (PERMANOVA) with 999 permutations, implemented through the adonis2 function in vegan. This analysis was conducted on both overall community data and individual species abundances, considering temperature, salinity, depth, and water mass type as explanatory variables. The interaction between temperature and salinity was also examined. Results were visualized using ggplot2 (version 3.3.5; Wickham et al. 2016).

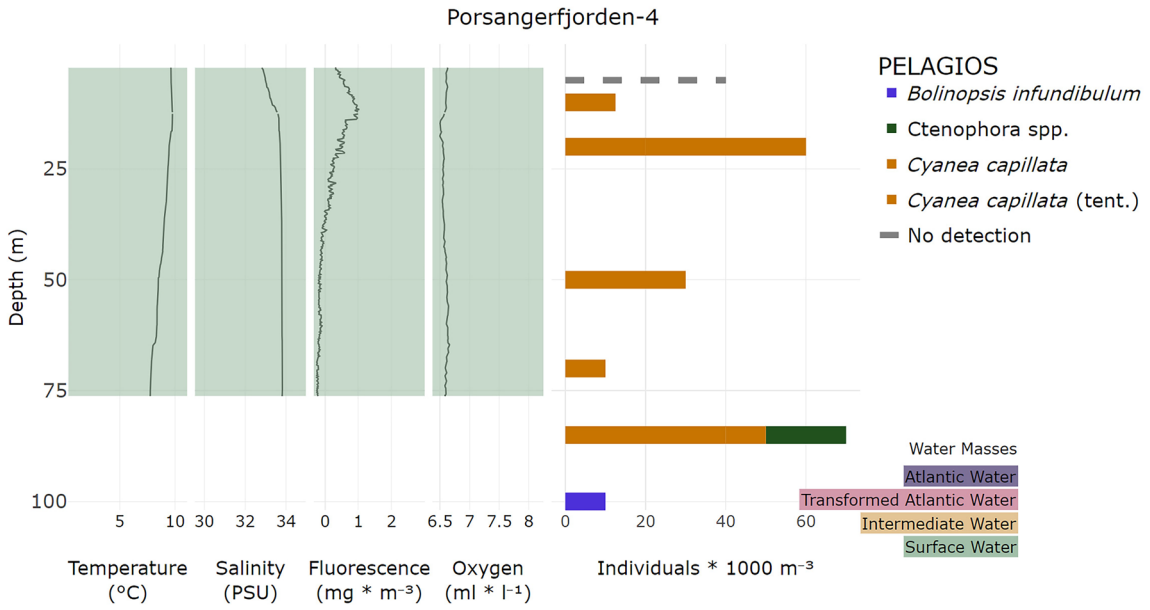

Fig. 4 (continued)

Results

Study areas and oceanography

At the stations Krossfjorden-1 and Kongsfjorden-3, CTD measurements revealed the presence of four distinct water masses: surface water (SW), intermediate water (IW), transformed Atlantic water (TAW), and Atlantic water (AW) (Fig. 4). In terms of depth distribution, surface and transitional waters were found down to 50 m in Krossfjorden-1, from below 50 to 170 m were Atlantic waters and the deepest level, up to 300 m depth, was represented by transformed Atlantic waters. At Krossfjorden-1, a sharp thermocline was observed between 20 and 50 m depth, where temperature dropped rapidly from approximately 6.5 to 4.8 °C, with a more gradual decrease to about 1 °C at 300 m depth. A corresponding halocline showed a rapid increase from about 31 PSU at the surface to 34.6 PSU at 50 m depth, gradually increasing to about 34.8 PSU at 300 m. Fluorescence displayed a pronounced peak at around 10 m depth. Oxygen concentration drops at the surface from 8 to 7 ml/l; then shows a slight increase of concentrations from 20 to 180 m and reaches a maximum zone of oxygen from 180 to 220 m (8.2 ml/l), then again drops to 7.5 ml/l near the bottom at 340 m. The water masses in Kongsfjorden-3 were dominated by a thicker layer of Atlantic water masses. This layer was found at depths between 50 and 220 m and was also mixed with intermediate water masses at depths between 40 and 70 m. The layer of transformed Atlantic water masses was thinner and situated between 240 and 270 m (Fig. 4). At Kongsfjorden-3, the CTD profile revealed a sharp thermocline between 20 and 60 m depth, where temperature dropped rapidly from approximately 6.8 to 5 °C, with a gradual decrease to about 1.7 °C at 270 m depth. A corresponding halocline showed a rapid increase from about 31.2 PSU at the surface to 34.7 PSU at 40 m depth, gradually increasing to about 34.85 PSU at 270 m. Fluorescence displayed a pronounced peak at around 12–14 m depth. Oxygen concentration showed an initial decrease from about 7.8 ml/l at the surface to approximately 7 ml/l at 40 m depth, followed by a slight increase to about 7.5 ml/l near the bottom at 270 m.

At the Van Mijenfjorden-3 station, where OFOS was deployed, the water masses were mainly represented by surface waters identified down to 75 m, while the deeper water masses were represented by transitional water masses (Fig. 4). The CTD profile at Van Mijenfjorden-3 showed a gradual thermocline extending from 40 m to about 75 m depth, where the temperature decreased from about 4.9 °C at 40 m to 1.6 °C at 75 m, with a slight further decrease to about 0.7 °C at the near bottom (85 m). A corresponding halocline showed a steady increase from about 29.7 PSU at the surface to 32.5 PSU at 40 m depth, with a more gradual increase down to deeper layers with values of 34.1 PSU (85 m). Fluorescence showed a broad peak between 5 and 40 m depth, indicating a deeper and more diffuse chlorophyll maximum compared to the other Svalbard stations.

Oxygen concentration remained relatively stable throughout the water column, with only a slight decrease from about 7.5 ml/l at the surface to 7 ml/l near the bottom.

At the station Hornsund-4 surveyed with PELAGIOS, we found three water masses, including surface water down to 40 m, followed by transitional water down to 125 m, which was the most extensive of its kind in all Svalbard fjords, and Atlantic water down to 210 m. The CTD profile at Hornsund-4 showed a sharp thermocline between 25 and 60 m depth, where the temperature dropped from about 5 to 3.3 °C. Below this, the temperature gradually decreased to about 32 °C at 210 m depth. A corresponding halocline showed a rapid increase from about 32 PSU at the surface to 34.5 PSU at 60 m depth, with a more gradual increase to about 34.7 PSU at 210 m. Fluorescence showed a pronounced peak at about 4–14 m depth, indicating a shallow chlorophyll maximum. Oxygen concentration showed a gradual decrease from about 7.6 ml/l at the surface to about 6.9 ml/l at the bottom at 210 m.

The water masses surveyed around the Barents Sea-1 station were largely represented by Atlantic water masses, with a thin layer of intermediate water masses in the upper 30 m (Fig. 4). These water masses were the warmest recorded during the expedition, reaching temperatures above 11 °C in the surface waters (Fig. 4; Fig. S1). A sharp thermocline was observed between 10 and 40 m depth, where the temperature dropped from about 10.3 to 6.1 °C. At the same time, this station had the highest surface chlorophyll-a concentrations of all stations observed at 30 m depth (fluorescence values reached 3 mg m^{-3}). These elevated chlorophyll-a concentrations are most likely the result of advection from the nearest phytoplankton bloom observed southwest of the site, which was detected one week prior to the sampling period (Fig. 5). The oxygen concentration showed a gradual decrease from the surface from about 6.4 to 6.8 ml/l near the bottom at 210 m.

Finally, we surveyed two stations in Porsangerfjorden, the largest fjord in northern Norway. The stations were mainly represented by surface water masses. Both stations were mainly represented by surface water masses. At Porsangerfjorden-3, the CTD profile showed a gradual thermocline from the surface to about 45 m, with temperatures decreasing from 8.7 to 3 °C, and further decreasing to 1.2 °C near the bottom at 70 m. The halocline showed a steady increase from 32.7 PSU at the surface to 33.5 PSU at 45 m, reaching 33.7 PSU at 70 m. Porsangerfjorden-4 showed a thermocline from 15 to 63 m, where temperatures decreased from 9.7 °C at the surface to 8.2 °C at 63 m, and a halocline between the surface layer and 13 m depth, where salinity increased from 32.8 to 33.6 PSU. Fluorescence patterns differed between the two stations, with Porsangerfjorden-3 showing a broad peak from the surface to 50 m, and Porsangerfjorden-4 showing a more pronounced, shallower peak at 10–15 m. Oxygen concentrations were slightly higher at Porsangerfjorden-3, ranging from 7 ml/l (from the surface layer to 30 m depth) to 7.5 ml/l (from 45 m to near the bottom), compared to uniform values of about 6.5 ml/l at Porsangerfjorden-3.

Biological data

In total, we recorded 14 taxonomic groups of GZ (Fig. 3), among which: *A. digitale* (63 observations), Appendicularia sp. (5 obs.), *Beroe* spp. (372 obs.), *B. infundibulum* (429 obs.), *C. capillata* (32 obs.). The rest of the taxa present in the Table 2. Taxon richness was highest at Hornsund-4 (9 taxa). Of the 7 stations in the study, unidentifiable ctenophores were present at 6, *Beroe* spp. were present at 5

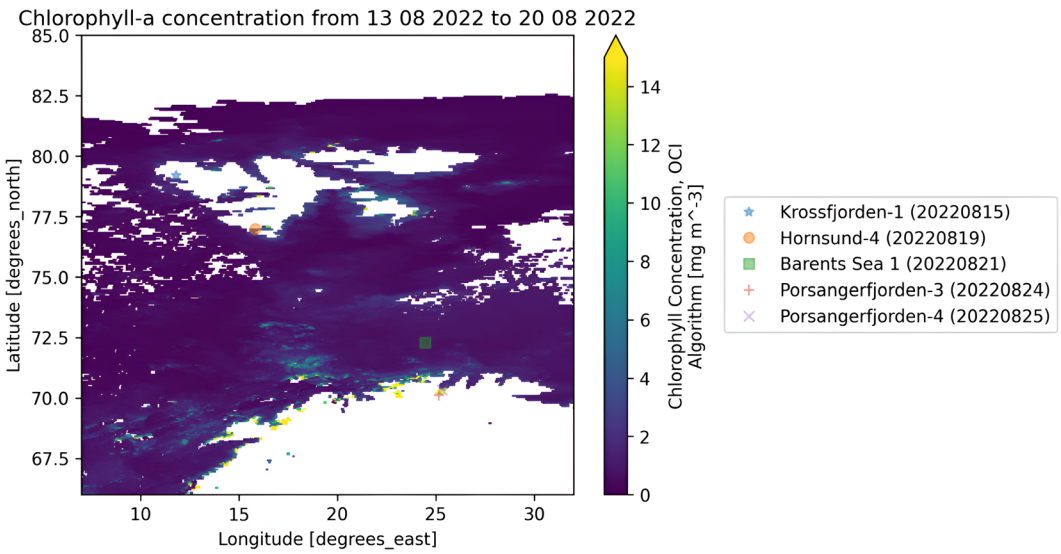

Fig. 5 Surface layer chlorophyll concentration data obtained from Aqua MODIS. Data retrieved from https://oceancolor.gsfc.nasa.gov

and *A. digitale* were present at 4. Most other taxa were only present at a single station (Fig. 4).

Regarding the observations of GZ derived from the PELAGIOS transects, the surveyed stations Barents Sea-1 (472 observations), Van Mijenfjorden-3 (262 observations), and Krossfjorden-1 (146 observations) had the highest numbers of observed organisms. The GZ fauna observed at station Barents Sea-1 was dominated by *B. infundibulum*, which accounted for most observations (90%). At station Van Mijenfjorden-3, the presence of *Beroe* spp. was dominant, accounting for 97% of the total observations at this OFOS station.

In the Krossfjorden–Kongsfjorden fjord system, we observed a significant differentiation between the types of gelatinous communities present in each of the two fjords. At Krossfjorden-1, we observed seven taxa of GZ, of which *Beroe* spp. (55 obs.) and *A. digitale* (37 obs.) were the most abundant. At Kongsfjorden-3, on the other hand, we observed an extremely limited taxon diversity (2 taxa observed), with a few observations of *A. digitale* and unidentified pandeid hydromedusae. At the same time, a large number of Chaetognatha sp. were observed (Havermans 2023). Regarding vertical zonation, station Krossfjorden-1 had the highest abundance and diversity of GZ in the near bottom layer. The highest abundance was observed at a depth of 300 m, where the total abundance was 920 ind. 1000 m^{-3}. Among them, the most abundant taxon was *Beroe* spp. (550 ind. 1000 m^{-3}). At depths of 50, 100, and 200 m, *A. digitale* was the dominant species, reaching a maximum abundance of 170 individuals per 1000 m^{-3} at 200 m (Fig. 4).

At the Van Mijenfjorden-3 station, where the OFOS was deployed, we observed a dominant presence of *Beroe* ctenophores. A total of 254 individuals of this taxon were recorded at the station. Some unidentifiable ctenophores and *M. ovum* (4 observations) were also present. Regarding the vertical distribution, almost all observations of *Beroe* spp. were below ~ 40 m. The distribution below this depth was homogeneous down to the bottom at 103 m. There were also occasional observations of unidentifiable Ctenophora, *M. ovum*, and a few *Solmundella bitentaculata* hydrozoans in the upper 40 m layer (Fig. 4).

At Hornsund-4, was characterized by the greatest taxon diversity of all surveyed stations, with 9 taxa found. The most abundant taxon included *Beroe* spp. (34 obs.), followed by *A. digitale* (14 obs.) and Ctenophora spp. (20 obs.). We observed a reduction in GZ abundance from the surface to depth. At this station we also found some *Pleurobrachia* sp. that were uniquely found at this station (3 obs.), as well as two individuals of *M. ovum*. At the near-surface depth of 20 m, there were 20 ind. 1000 m^{-3}, and at 180 m depth, the number of individuals increased to 410 ind. 1000 m^{-3}. At a depth of 180 m, Ctenophora spp. (100 ind. 1000 m^{-3}) and *Beroe* spp. (240 ind. 1000 m^{-3}) were the most abundant species. *A. digitale* individuals were evenly distributed throughout the water column, with the greatest presence at 100 m (60 ind. 1000 m^{-3}), but were absent from the upper 20 and 50 m (Fig. 4).

At the Barents Sea-1 station, we recorded a large number of the lobate ctenophore *B. infundibulum*. This species was predominantly aggregated in the 100 m depth layer, with some extension into the 150 m layer (observed during both the initial descent to 200 m and subsequent ascent of the transect). At 100 m we found the densest population of all GZ recorded, with more than 2600 ind. 1000 m^{-3}. It is noteworthy that this species was strongly associated with these depth layers and was less abundant in other layers. At this station, we also recorded a small number of *C. capillata* in the upper 50 m (10 ind. 1000 m^{-3}), as well as *Beroe* spp. which were mainly found at 200 m depth (140 ind. 1000 m^{-3}; Fig. 4).

Two stations surveyed with PELAGIOS in Porsangerfjorden (-3 and -4) had rather different patterns of GZ observations. *C. capillata* was the most abundant taxon recorded at both stations with a total of 30 identified individuals (14 directly observed and 16 identified from the presence of tentacles). The highest abundance was found at 20 m depth with 40 ind. 1000 m^{-3}. At station Porsangerfjorden-3, which was closer to the mouth of the fjord, a small number of *C. capillata* were found on the surface, as well as *M. octocostatum* at a depth of 20 m with 40 ind. 1000 m^{-3} (Fig. 4). In contrast, at the deeper station Porsangerfjorden-4, the dominance of *C. capillata* was more pronounced throughout the water column. Occasional records were also made of *A. digitale*, Physonectae spp., *Beroe* spp., and *B. infundibulum*.

Table 2 Taxonomic groups of gelatinous zooplankton (GZ) recorded during the HE605 expedition and number of observations

Taxonomic group	Observations
Bolinopsis infundibulum	429
Beroe spp.	372
Aglantha digitale	63
Ctenophora spp.	46
Cyanea capillata	32
Cydippida spp.	17
Mertensia ovum	16
Euplokamis sp.	9
Physonectae spp.	7
Appendicularia sp.	5
Pandeidae sp.	5
Melicertum octocostatum	4
Pleurobrachia sp.	3
Trachymedusae sp.	1

When examining the association between various taxa of GZ and the identified water masses during the optical transects, we found that the transformed Atlantic and Atlantic waters were characterized by the highest abundance of GZ (Fig. 6). Taxa such as *Euplokamis* sp., *Beroe* spp., *A. digitale* had the highest abundance in the transformed Atlantic and Atlantic waters, while *B. infundibulum* was predominantly associated with the Atlantic waters. Conversely, colder, intermediate water masses were characterized by the lowest abundance of GZ, but higher taxa diversity (Fig. 6).

Statistical analysis

A Principal Component Analysis (PCA) was performed on the Hellinger-transformed species abundance data to examine patterns in community composition across different water masses (Fig. 7). The first two principal components accounted for 31.02 and 15.88% of the total variance, respectively. The PCA biplot revealed a partial separation of Atlantic Water and Transformed Atlantic Water samples along PC1, while Intermediate Water and Surface Water samples showed more dispersion along both axes (Fig. 7).

Species richness varied across water masses, though the differences were not statistically significant (ANOVA, $F3,21 = 2.822$, $p = 0.0636$). Total GZ abundance also differed between water masses, but these differences were not statistically significant (ANOVA, $F3,21 = 2.268$, $p = 0.11$).

Permutational multivariate analysis of variance (PERMANOVA) was used to assess the effects of temperature, salinity, depth, and water mass type on overall community structure and individual species abundances (Table 3). Salinity emerged as a significant predictor of total abundance (pseudo-$F = 4.47$, $p = 0.042$). However, temperature (pseudo-$F = 3.21$, $p = 0.086$), the interaction between temperature and salinity (pseudo-$F = 3.59$, $p = 0.071$), depth (pseudo-$F = 1.12$, $p = 0.387$), and dominant water masses (pseudo-$F = 2.82$, $p = 0.063$) did not show statistically significant effects on species richness or total abundance.

Discussion

In our study area, we recorded more than 1000 individual observations of GZ that could be assigned to 14 taxonomic groups. The most dominant taxa encountered during the pelagic surveys were *A. digitale*, *Beroe* spp. and *B. infundibulum*. We found large aggregations of *Beroe* spp. in a Svalbard fjord (Van Mijenfjorden) and of *B. infundibulum* in the open waters of the Barents Sea. The water masses with the highest GZ abundances were the transformed Atlantic waters, while we observed the highest species richness in intermediate water masses. Our results provide a better picture of the patterns of ctenophore aggregations and can be used as a basis for further monitoring of changing Arctic ecosystems.

Diversity patterns

Our data showed that GZ taxa composition at Krossfjorden was typical of fjords in Svalbard in comparison to previous studies (Bandara et al. 2016; Hop et al. 2019). In particular, we recorded a high prevalence of gelatinous taxa such as *Beroe* spp., *A. digitale* and *M. ovum*, known to be abundant in Arctic regions (Kosobokova et al. 2011). In contrast, the Kongsfjorden station was dominated by Chaetognatha sp., with only a few observations of hydrozoan taxa (*A. digitale* and Pandeidae sp.). Our results are consistent with seasonal peaks in Chaetognatha sp. abundance, typically observed in late summer and autumn (Grigor et al. 2014). It has been shown in Billefjorden, another fjord in the Svalbard archipelago, that Chaetognatha sp. may be competitors of *A. digitale* and *M. ovum* for their main prey, Calanus spp., although further studies on gut content have been suggested to verify this (Bandara et al. 2016). This, together with other environmental factors not measured here, could be a potential explanation for the absence of *M. ovum* and low abundance of *A. digitale* at the Kongsfjorden station, as previously suggested by Bandara et al. (2016). With respect to the depth distribution in the fjords of Svalbard, the highest abundance of taxa found near the bottom is in line with the previously reported descent to deeper waters of gelatinous communities in late August in the area of Fram Strait (Pantiukhin et al. 2023). The observed aggregations in the Svalbard fjord system might be driven by *Calanus* spp., the food source for some GZ species, which are known to migrate to deeper waters to overwinter in August (Pages and Gonzalez 1997; Purcell et al. 2010; Hop et al. 2019). In Porsangerfjorden, we found large numbers of *C. capillata*. At two stations in this fjord, at depths where *C. capillata* abundance was high, other GZ taxa were virtually absent, except for a few specimens of *Melicertum octocostatum*. Since *C. capillata* is known to feed on other types of GZ (Hosia and Titelman 2011; Titelman et al. 2007; Båmstedt et al. 1997), its predation pressure in the fjord may be considerable. We did not record the newly recorded species *Periphylla periphylla* in the Svalbard fjords, although this species has a fairly wide distribution from the fjords of Norway to Svalbard (Geoffroy et al. 2018). We however have recorded a dead individual during a transect with the OFOS in Hornsund fjord.

With regard to the association of zooplankton with different water masses, it has been hypothesized that Atlantic water masses bring more diverse and abundant communities to the Arctic (Hop et al. 2019). As mentioned before, the opposite trend has been shown for GZ communities inhabiting the shelf areas off Svalbard and Fram Strait (Mańko et al. 2020; Pantiukhin et al. 2023). These studies found higher

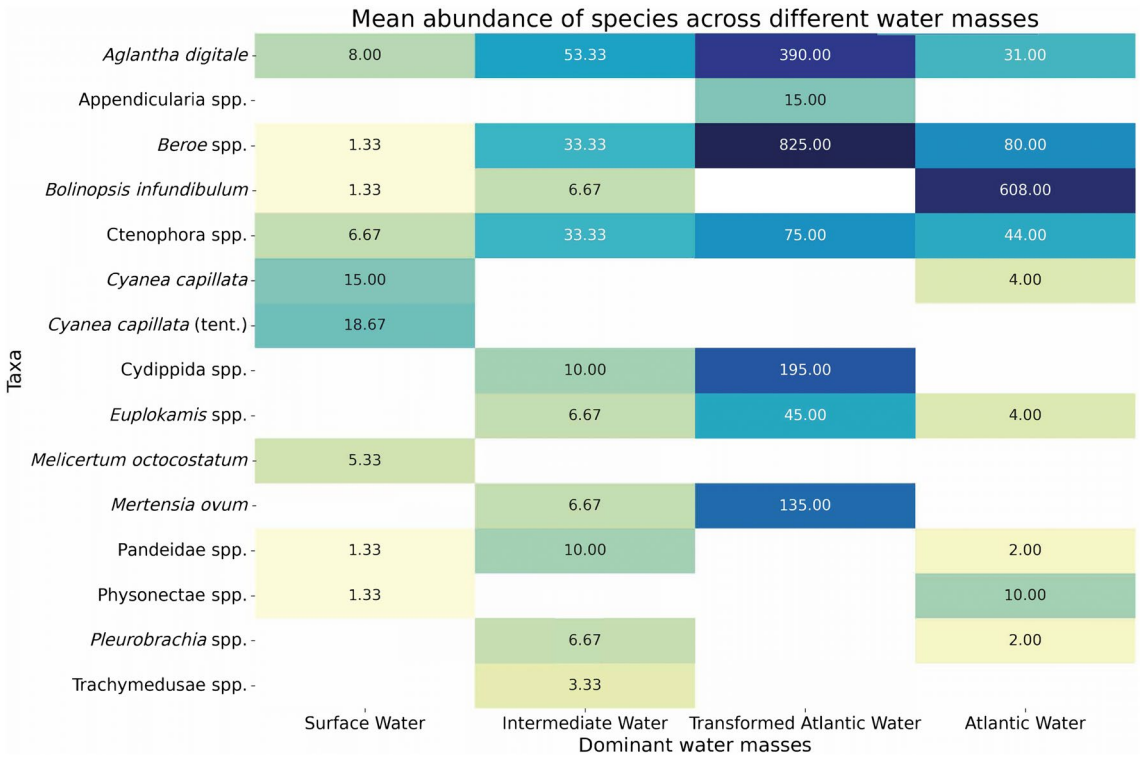

Fig. 6 Mean abundance of species across different water masses (ind. 1000 m^{-3})

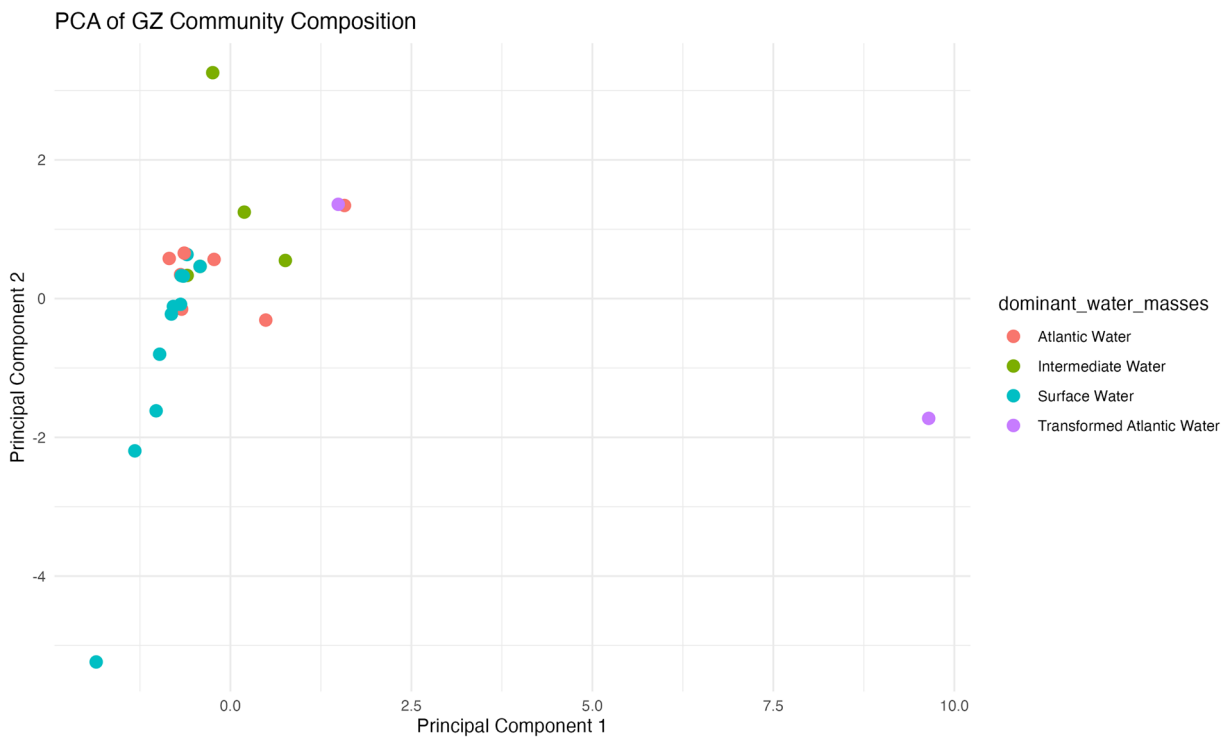

Fig. 7 Principal component analysis (PCA) of Gelatinous Zooplankton (GZ) community composition in the Arctic region

Table 3 The 2- and 3-way PERMANOVA tests for total abundance, species richness, and most abundant taxa

Factor	Species richness	Abundance	*Aglantha digitale*	*Beroe* spp.	*Bolinopsis infundibulum*	Ctenophora spp.	*Cyanea capillata*	Cydippida spp.	*Mertensia ovum*
Temperature	1.96	1.76	6.71*	3.77	0.01	2.05	7.56*	3.34	2.96
Salinity	1.76	5.01*	4.07*	2.25	1.80	3.49	6.68*	1.29	1.18
Temperature x Salinity	2.00	2.08	8.42*	4.69*	0.01	2.21	9.74*	4.00	3.47
Depth	1.06	1.26	0.97	62.93*	0.45	2.11	1.13	96.13	96.47
dominant_water_masses	1.84	3.31*	18.37*	5.15*	1.12	1.41	1.39	8.63*	6.11*

The asterisks represent statistically significant results ($p < 0.05$)

taxon richness in the Arctic and intermediate waters, while a higher GZ abundance was characteristic of the Atlantic water masses (Mańko et al. 2020; Pantiukhin et al. 2023). Our observations may corroborate these GZ studies, as we observed the highest GZ diversity in the colder, intermediate water masses, while the different types of warmer (Atlantic) waters yielded the highest abundances of GZ, but with lower diversity. The fact that Hornsund, the West Svalbard fjord generally known to be still an Arctic-type fjord (Jakacki et al. 2017), harbored the highest taxon richness of all stations, also confirms this observed trend for GZ.

Our statistical analyses provide some support for these observations, although the results are not definitive. The Principal Component Analysis (PCA) revealed a trend towards separation of Atlantic Water, Transformed Atlantic Water and Intermediate Water samples, suggesting some distinction in GZ community composition between these water masses. While the PERMANOVA did not show statistically significant effects of water mass type on species richness or total abundance, the relatively low p-value (0.063) hints at a potential relationship that might be clarified with a larger dataset.

Ctenophores aggregations and their potential drivers

Bolinopsis infundibulum

The highest abundances of GZ recorded with PELAGIOS at the surveyed stations was for the species *B. infundibulum*. This aggregation was observed at the Barents Sea station-1, peaking at 2670 ind. 1000 m^{-3} at a depth of 100 m. Such large aggregations of *B. infundibulum* have been previously described in the Irish Sea (Nagabhushanam 1959) and in the fjords of northern Norway (Båmstedt and Martinussen 2015). In particular, Båmstedt and Martinussen (2015), using ROV, estimated similarly high abundances in Halsafjorden, with abundances of *B. infundibulum* up to 2000 ind. 1000 m^{-3}. Aggregations of GZ are rarely caused by a single environmental or biotic driver, but rather by multiple factors (Dawson and Hamner 2009). One of the most documented factors driving aggregations of *B. infundibulum* is prey abundance (Båmstedt and Martinussen 2015). *B. infundibulum* can be very efficient at exploiting changes in environmental conditions and prey availability, primarily feeding on small crustaceans (Gamble 1974; Falkenhaug 1996). Its biomass has been reported to triple in just two weeks (Falkenhaug 1996), while its feeding response to prey abundance is linear (under experimental conditions; Båmstedt and Martinussen 2015).

To investigate the potential origin of such large aggregations, we further explored the chlorophyll-a concentrations from satellite data. At the Barents Sea station we documented the highest chlorophyll-a concentrations in the epipelagic layer among all stations studied during the PELAGIOS deployments. A study by Toyokawa et al. (2003) indicated that *Bolinopsis infundibulum* likely relies on surface photosynthetic products for nutrition, which might suggest a connection to surface photosynthetic production. By investigating the origin of the high chlorophyll-a concentrations at the Barents Sea station, we found, based on satellite data, a phytoplankton bloom a few kilometers away that occurred one week prior to sampling at this station. Whether the large numbers of *Bolinopsis* were attracted to this bloom, and the potentially high zooplankton biomass associated with it, and whether such large aggregations can extend over the few kilometers where the phytoplankton blooms could be observed, remain open questions. Further long-term optical studies should provide more insight.

Surprisingly, we found the aggregation of B. infundibulum at a depth of 100 m, which extended down to 150 m (based on information from the descent phase), while abundances were significantly lower at the surface and in the deeper layers. *B. infundibulum* is known to be eurybathic and its occurrence at different depths is closely related to seasonality (Toyokawa et al. 2003). This species has been

reported near the coast of Murman, south of the Barents Sea, where it reaches its maximum abundance in shallow waters in July–August and begins to descend to the deep waters by the end of July (Kamshilov 1960). One of the explanations for such a dense aggregation at deeper depths observed in our study could be linked to predator avoidance behavior, combined with feeding patterns and seasonal vertical migrations. *B. infundibulum* is known to occupy a rather low trophic level (Toyokawa et al. 2003) and is preyed upon by many organisms, including Atlantic cod (*Gadus morhua*), *Beroe* spp., and *Cyanea* species (Falkenhaug 1996). In the fjords of mainland Norway, *B. infundibulum* has been shown to reach its peak abundance in early May, with a further drastic decline when *Beroe cucumis* becomes more abundant (Båmstedt and Martinussen 2015). Interestingly, at this station, we only observed *Beroe* ctenophores near oxygenated depths around 200 m. Although the oxygen consumption of *Beroe* has been shown to be lower than that of *B. infundibulum*, *Beroe* requires more oxygen for hunting and digestion than does *B. infundibulum*, which uses a more passive feeding mode (Gyllenberg and Greve 1979). Thus, *B. infundibulum* may either actively avoid predation by *Beroe* spp. in the more hypoxic zones of the upper water column, or be largely consumed by *Beroe* in the higher oxygen zones, leading to their absence. In our case, such predation pressure could be the reason for the drastic decrease in *B. infundibulum* abundance from 100 to 200 m, where we observed *Beroe* ctenophores with more than 140 ind. 1000 m^{-3}. On the other hand, the absence of *B. infundibulum* from surface zones could be due to either active avoidance of, or predation by, *C. capillata*. *C. capillata* is known to be a predator of *B. infundibulum*, which is an essential food source for its development (Båmstedt et al. 1997).

Beroe spp.

At Van Mijenfjorden station, we observed a large aggregation of *Beroe* spp. during the ascent of the OFOS system at the end of a seafloor survey. Within the 7 min of ascent, we documented more than 254 individuals of this species. Unfortunately, due to the challenges of quantifying the water volumes surveyed during this ascent, we cannot estimate the exact abundance of these species, but numbers range somewhere between 3000 and 5000 ind. 1000 m^{-3}. At this station, the aggregation of the *Beroe* ctenophores was situated in the oxygenated part of the water column where oxygen concentrations were above 7.4 ml/l. It is known that *Beroe* species are less tolerant to low-oxygen environments or oxygen-depleted waters in comparison to other gelatinous taxa (Breitburg et al. 2003). In the North Atlantic, off Cape Verde, *Beroe* species were shown to have a discontinuous distribution along the water column, explained by the avoidance of oxygen minimum zones, which shows that oxygen is an important factor for species belonging to this genus, compared to other jellyfish and ctenophores (Hoving et al. 2020). While their oxygen consumption in the resting state is known to be comparable to that of other ctenophores, *Beroe* species exhibit more oxygen-demanding feeding habits (Gyllenberg and Greve 1979). Their oxygen consumption increases significantly during digestion and swallowing of prey, which may potentially explain their aggregation around oxygen-rich zones (Gyllenberg and Greve 1979). While *Beroe* spp. were not always found at the depths of maximum oxygen concentration, they were generally observed in relatively oxygen-rich zones below the oxycline. This suggests that while oxygen availability is an important factor, it may not be the sole determinant of their vertical distribution.

Optical surveys to assess GZP abundances

Different types of sampling methods, including trawls, nets, and optical methods, are known to produce different results on the abundance and taxonomic composition of GZ in the surveyed environment (Hosia et al. 2017). The PELAGIOS system provides in-situ video observations, capturing detailed data on organisms > ~ 1 cm in size (Hoving et al. 2019). However, optical surveys, including PELAGIOS, face challenges in species-level identification for several taxa, leading to the classification of organisms into broader taxonomic groups. This issue is particularly noticeable in the upper layers of the water column, where high concentrations of particulate organic carbon and sunlight reduce the effective observation distance, exacerbating classification difficulties. This bias is evident for the Ctenophora, where the transparency of ctenophores complicates identification. To mitigate potential biases in abundance estimates, we employed a conservative approach in our annotations, focusing only on organisms with distinct features characteristic of each taxonomic group. However, as noted by Neitzel et al. (2021), estimating abundance of larger fauna with PELAGIOS requires further calibration efforts, as these organisms may be detected at greater distances from the camera compared to smaller ones.

Despite these challenges, PELAGIOS has demonstrated robust data collection for taxa highly sensitive to fragmentation when sampled by traditional net methods (e.g., Polychaeta, Ctenophora, Appendicularia; Christiansen et al. 2018; Hoving et al. 2019; Neitzel et al. 2021). For example, in the Barents Sea, PELAGIOS recorded high abundances of ctenophores (mainly *B. infundibulum*), with average values of 670 ind. 1000 m^{-3} over the entire water column, and values over 2670 ind. 1000 m^{-3} at 100 m depth, which net sampling missed (Havermans 2023). Additionally, the larger observation volume of PELAGIOS compared to vertical Multi-net hauls allows for higher detection rates of large, sparsely distributed species such as *Cyanea capillata*. Both

Multinet sampling and PELAGIOS have limitations and advantages, and their complementary use can offer a more comprehensive understanding of GZ diversity and abundance in Arctic ecosystems.

Conclusion

Our work provides an overview on the diversity, community structure and vertical distribution of GZ in different Arctic fjord and shelf systems. Using the towed video system PELAGIOS, we observed that GZ are characterized by higher abundances in the Atlantic water masses but are more diverse in the intermediate Arctic waters. We also detected large aggregations of Ctenophora species, *Beroe* spp. inshore in Van Mijenfjorden and *B. infundibulum* offshore in the Barents Sea. *B. infundibulum* aggregations showed a clear zonation with depth and probably extended over many kilometers, although the spatial extent of these aggregations remains uncertain and requires further investigation. For a more complete understanding of the spatial and temporal dynamics of GZ aggregations in future studies, the use of autonomous underwater vehicles with video systems may allow study of these aggregations while moving close to them.

Supplementary Information The online version contains supplementary material available at https://doi.org/10.1007/s00300-024-03306-0.

Acknowledgements This study has been conducted in the framework of the Helmholtz Young Investigator Group "ARJEL – Arctic Jellies" with the project number VH-NG-1400, led by CH and funded by the Helmholtz Society and the Alfred Wegener Institute Helmholtz Centre for Polar and Marine Research. It was further supported by the Helmholtz Research Programme "Changing Earth – Sustaining our Future" Topic 6, Subtopic 6.1. HJH was funded by the Emmy Noether Junior Research Group by the Deutsche Forschungsgemeinschaft e. V. (DFG) under grant HO 5569/2-1. Data for this manuscript was produced as part of the HE605 RISING project (PI Havermans) with the following Heincke project ID: AWI_HE605_00. Research was conducted under the Norwegian License No. 819/2022 and Research in Svalbard project with RIS ID 11915. We are grateful to Hendrik Hampe (GEOMAR) who was responsible for the PELAGIOS and OFOS deployments during HE605. We greatly thank R/V Heincke's Master Haye Diecks and the ship's crew for their skillful support during the expedition, as well as AWI logistics and ship's coordination for their assistance with expedition planning.

Author contributions This study was conceived by CH and DP. CH applied for shiptime and led the fieldwork. AH and JJSA contributed to the fieldwork. HJH contributed to the ship time application and provided instrumentation and personnel for carrying out the optical surveys. DP carried out all the optical annotations, with input of AH and JJSA. DP performed all analyses, with methodological input of CH. DP was responsible for writing, with extensive input of CH, and further contributions and corrections from all other authors resulting in the final version.

Funding Open Access funding enabled and organized by Projekt DEAL. Open Access funding enabled and organized by Projekt DEAL.

Data availability All data generated or analyzed during this study are included in this published article. No datasets were generated or analysed during the current study.

Declarations

Conflict of interest The authors declare no competing interests.

References

Alfred Wegener Institute Helmholtz Centre for Polar and Marine Research (2017) Research vessel HEINCKE operated by the Alfred-Wegener-Institute. J Large-Scale Res Facil 3:A120

Alldredge AL (1984) The quantitative significance of gelatinous zooplankton as pelagic consumers. In Flows of energy and materials in marine ecosystems: theory and practice, pp 407–433

Arai MN (1992) Active and passive factors affecting aggregations of hydromedusae: a review. Sci Mar 56(2):99–108

Båmstedt U, Martinussen MB (2015) Ecology and behavior of Bolinopsis infundibulum (Ctenophora; Lobata) in the Northeast Atlantic. Hydrobiologia 759:3–14

Båmstedt U, Ishii H, Martlnussen MB (1997) Is the scyphomedusa Cyanea capillata (L.) dependent on gelatinous prey for its early development? Sarsia 82:269–273

Bandara K, Varpe Ø, Søreide JE, Wallenschus J, Berge J, Eiane K (2016) Seasonal vertical strategies in a high-Arctic coastal zooplankton community. Mar Ecol Prog Ser 555:49–64

Batistić M, Kršinić F, Jasprica N, Carić M, Viličić D, Lučić D (2004) Gelatinous invertebrate zooplankton of the South Adriatic: species composition and vertical distribution. J Plankton Res 26:459–474

Bayha KM, Richard Harbison G, Mcdonald JH, Gaffney PM (2004) Preliminary investigation on the molecular systematics of the invasive ctenophore Beroe ovata. Aquatic Invasions in the Black, Caspian, and Mediterranean Seas: the Ctenophores Mnemiopsis leidyi and Beroe in the Ponto-Caspian and other Aquatic Invasions. Springer, Netherlands, pp 167–175

Błaszczyk M, Jania J, Kolondra L (2013) Fluctuations of tidewater glaciers in Hornsund Fjord (Southern Svalbard) since the beginning of the 20th century

Breitburg DL, Adamack A, Rose KA, Kolesar SE, Decker B, Purcell JE, Cowan JH (2003) The pattern and influence of low dissolved oxygen in the Patuxent River, a seasonally hypoxic estuary. Estuaries 26:280–297

Brotz L, Cheung WW, Kleisner K, Pakhomov E, Pauly D (2012) Increasing jellyfish populations: trends in large marine ecosystems. In: Jellyfish Blooms IV: Interactions with humans and fisheries, pp 3–20

Choy CA, Haddock SH, Robison BH (2017) Deep pelagic food web structure as revealed by in situ feeding observations. Proc R Soc B 284:20172116

Christiansen S, Hoving HJ, Schütte F, Hauss H, Karstensen J, Körtzinger A, Kiko R (2018) Particulate matter flux interception in oceanic mesoscale eddies by the polychaete *Poeobius* sp. Limnol Oceanogr 63(5):2093–2109

Condon RH, Duarte CM, Pitt KA, Robinson KL, Lucas CH, Sutherland KR, Graham WM (2013) Recurrent jellyfish blooms are a consequence of global oscillations. Proc Natl Acad Sci USA 110:1000–1005

Cottier F, Tverberg V, Inall M, Svendsen H, Nilsen F, Griffiths C (2005) Water mass modification in an Arctic fjord through cross-shelf exchange: the seasonal hydrography of Kongsfjorden, Svalbard. J Geophys Res Oceans 110:C12

Cottier FR, Nilsen F, Skogseth R, Tverberg V, Skarðhamar J, Svendsen H (2010) Arctic fjords: a review of the oceanographic environment and dominant physical processes. Geol Soc Lond Spec Publ 344:35–50

David C, Lange B, Rabe B, Flores H (2015) Community structure of under-ice fauna in the Eurasian central Arctic Ocean in relation to environmental properties of sea-ice habitats. Mar Ecol Prog Ser 522:15–32

Dawson MN, Hamner WM (2009) A character-based analysis of the evolution of jellyfish blooms: adaptation and exaptation. In: Jellyfish blooms: causes, consequences, and recent advances: proceedings of the second international jellyfish blooms symposium, held at the Gold Coast, Queensland, Australia, 24–27 June, 2007. Springer Netherlands, pp 193–215

Falkenhaug T (1996) Distributional and seasonal patterns of ctenophores in Malangen, northern Norway. Mar Ecol Prog Ser 140:59–70

Fernández-Alías A, Marcos C, Perez-Ruzafa A (2021) Larger scyphozoan species dwelling in temperate, shallow waters show higher blooming potential. Mar Pollut Bull 173:113100

Fox-Kemper B, Hewitt HT, Xiao C, Aðalgeirsdóttir G, Drijfhout SS, Edwards TL, Golledge NR, Hemer M, Kopp RE, Krinner G, Mix A, Notz D, Nowicki S, Nurhati IS, Ruiz L, Sallée JB, Slangen ABA, Yu Y (2021) Ocean, cryosphere and sea level change. In: Climate change 2021: the physical science basis. Contribution of working group I to the sixth assessment report of the intergovernmental panel on climate change. Cambridge University Press, Cambridge, pp 1211–1362

Gamble JC (1974) Preliminary observations on the feeding of Bolinopsis infundibulum. In: International council for the exploration of the sea, committee meeting, vol 50, p 14

Geoffroy M, Berge J, Majaneva S, Johnsen G, Langbehn TJ, Cottier F, Last K (2018) Increased occurrence of the jellyfish Periphylla periphylla in the European high Arctic. Polar Biol 41:2615–2619

Graham WM, Pagès F, Hamner WM (2001) A physical context for gelatinous zooplankton aggregations: a review. In: Jellyfish blooms: ecological and societal importance: proceedings of the international conference on jellyfish blooms, held in Gulf Shores, Alabama, 12–14 January 2000. Springer Netherlands, pp 199–212

Grigor JJ, Søreide JE, Varpe Ø (2014) Seasonal ecology and life-history strategy of the high-latitude predatory zooplankter Parasagitta elegans. Mar Ecol Prog Ser 499:77–88

Gyllenberg G, Greve W (1979) Studies on oxygen uptake in ctenophores. In: *Annales Zoologici Fennici*. Finnish Academy of Sciences, Societas Scientiarum Fennica, Societas pro Fauna et Flora Fennica and Societas Biologica Fennica Vanamo, pp 44–49

Hamner WM, Dawson MN (2009) A review and synthesis on the systematics and evolution of jellyfish blooms: advantageous aggregations and adaptive assemblages. Hydrobiologia 616:161–191

Hamner WM, Schneider D (1986) Regularly spaced rows of medusae in the Bering Sea: Role of Langmuir circulation 1. Limnol Oceanogr 31:171–176

Hari Praved P, Morandini AC, Maronna MM, Suhaana MN, Jima M, Aneesh BP, Jayachandran PR (2021) Report of Mauve Stinger Pelagia cf. noctiluca (Cnidaria: Scyphozoa) bloom from Northeastern Arabian Sea (NEAS). Thalassas 37:569–576

Havermans C (2023) The role and range boundaries of gelatinous zooplankton in the rapidly changing Arctic marginal seas. Cruise report R/V Heincke HE605

Hop H, Assmy P, Wold A, Sundfjord A, Daase M, Duarte P, Vihtakari M (2019) Pelagic ecosystem characteristics across the Atlantic water boundary current from Rijpfjorden, Svalbard, to the Arctic Ocean during summer (2010–2014). Front Mar Sci 6:181

Hosia A, Titelman J (2011) Intraguild predation between the native North Sea jellyfish Cyanea capillata and the invasive ctenophore Mnemiopsis leidyi. J Plankton Res 33:535–540

Hosia A, Falkenhaug T, Baxter EJ, Pagès F (2017) Abundance, distribution and diversity of gelatinous predators along the northern Mid-Atlantic Ridge: a comparison of different sampling methodologies. PLoS ONE 12:e0187491

Hoving HJ, Christiansen S, Fabrizius E, Hauss H, Kiko R, Linke P, Körtzinger A (2019) The Pelagic In situ Observation System (PELAGIOS) to reveal biodiversity, behavior, and ecology of elusive oceanic fauna. Ocean Sci 15:1327–1340

Hoving HJT, Neitzel P, Hauss H, Christiansen S, Kiko R, Robison BH, Körtzinger A (2020) In situ observations show vertical community structure of pelagic fauna in the eastern tropical North Atlantic off Cape Verde. Sci Rep 10:21798

Ingvaldsen RB, Assmann KM, Primicerio R, Fossheim M, Polyakov IV, Dolgov AV (2021) Physical manifestations and ecological implications of Arctic Atlantification. Nat Rev Earth Environ 2:874–889

Jakacki J, Przyborska A, Kosecki S, Sundfjord A, Albretsen J (2017) Modelling of the Svalbard fjord Hornsund. Oceanologia 59:473–495

Jakobsen T, Ozhigin VK (2011) The Barents Sea: ecosystem, resources, management-half a century of Russian-Norwegian cooperation

Johansson ML, Shiganova TA, Ringvold H, Stupnikova AN, Heath DD, MacIsaac HJ (2018) Molecular insights into the ctenophore genus Beroe in Europe: new species, spreading invaders. J Hered 109:520–529

Jucker MN, Havermans C (2022) The phylogeography of two Beroe species in the Arctic Ocean based on one mitochondrial and one ribosomal marker

Kamshilov MM (1960) Biology of ctenophores off Murman. ICES CM 5

Kosobokova KN, Hopcroft RR, Hirche HJ (2011) Patterns of zooplankton diversity through the depths of the Arctic's central basins. Mar Biodivers 41:29–50

Langenkämper D, Zurowietz M, Schoening T, Nattkemper TW (2020) Corrigendum: BIIGLE 2.0-browsing and annotating large marine image collections. Front Mar Sci 7:617268

Larson RJ (1986) Water content, organic content, and carbon and nitrogen composition of medusae from the northeast Pacific. J Exp Mar Biol Ecol 99:107–120

Long AP, O'Donnell C, Haberlin D, Lawton C, Doyle TK (2020) A novel platform for monitoring gelatinous mesozooplankton: the high-speed Gulf VII sampler quantifies gelatinous mesozooplankton similar to a ring net. Limnol Oceanogr Methods 18:696–706

Luo JY, Condon RH, Stock CA, Duarte CM, Lucas CH, Pitt KA, Cowen RK (2020) Gelatinous zooplankton-mediated carbon flows in the global oceans: a data-driven modeling study. *Global Biogeochem Cycles* 34:e2020GB006704

Lüskow F, Nöthig EM, Wento I, Hoving HJT (2021) Gelatinous and soft-bodied zooplankton in the Northeast Pacific Ocean: organic, elemental, and energy contents. Mar Ecol Prog Ser 665:19–35

Mańko MK, Gluchowska M, Weydmann-Zwolicka A (2020) Footprints of Atlantification in the vertical distribution and diversity of gelatinous zooplankton in the Fram Strait (Arctic Ocean). Prog Oceanogr 189:102414

Melsom A, Counillon F, LaCasce JH, Bertino L (2012) Forecasting search areas using ensemble ocean circulation modeling. Ocean Dyn 62:1245–1257

Mills CE (2001) Jellyfish blooms: are populations increasing globally in response to changing ocean conditions? Hydrobiologia 451:55–68

Nagabhushanam AK (1959) Feeding of a ctenophore, Bolinopsis infundibulum (OF Müller). Nature 184:829–829

Neitzel P, Hosia A, Piatkowski U, Hoving HJ (2021) Pelagic deep-sea fauna observed on video transects in the southern Norwegian Sea. Polar Biol 44:887–898

Oksanen J, Simpson G, Blanchet F, Kindt R, Legendre P, Minchin P, O'Hara R, Solymos P, Stevens M, Szoecs E, Wagner H, Barbour M, Bedward M, Bolker B, Borcard D, Carvalho G, Chirico M, De Caceres M, Durand S, Evangelista H, FitzJohn R, Friendly M, Furneaux B, Hannigan G, Hill M, Lahti L, McGlinn D, Ouellette M, Ribeiro Cunha E, Smith T, Stier A, Ter Braak C, Weedon J (2024) vegan: Community Ecology Package. R package version 2.7-0, https://github.com/vegandevs/vegan, https://vegandevs.github.io/vegan/

Pages F, Gonzalez SR (1997) Diet of the gelatinous zooplankton in Hardangerfjord (Norway) and potential predatory impact by Aglantha digitale (Trachymedusae). Oceanogr Lit Rev 3:237

Pantiukhin D, Verhaegen G, Kraan C, Jerosch K, Neitzel P, Hoving HJT, Havermans C (2023) Optical observations and spatio-temporal projections of gelatinous zooplankton in the Fram Strait, a gateway to a changing Arctic Ocean. Front Mar Sci 10:987700

Pantiukhin D, Verhaegen G, Havermans C (2024) Pan-Arctic distribution modeling reveals climate-change-driven poleward shifts of major gelatinous zooplankton species. Limnol Oceanogr

Picheral M, Catalano C, Brousseau D, Claustre H, Coppola L, Leymarie E, Stemmann L (2022) The underwater vision profiler 6: an imaging sensor of particle size spectra and plankton, for autonomous and cabled platforms. Limnol Oceanogr Methods 20:115–129

Polyakov IV, Alkire MB, Bluhm BA, Brown KA, Carmack EC, Chierici M, Wassmann P (2020) Borealization of the Arctic Ocean in response to anomalous advection from sub-Arctic seas. Front Mar Sci 7:491

Purcell JE (2005) Climate effects on formation of jellyfish and ctenophore blooms: a review. J Mar Biol Assoc UK 85:461–476

Purcell JE, Hopcroft RR, Kosobokova KN, Whitledge TE (2010) Distribution, abundance, and predation effects of epipelagic ctenophores and jellyfish in the western Arctic Ocean. Deep Sea Res Part II 57:127–135

R Core Team (2023) R: A language and environment for statistical computing. R Foundation for Statistical Computing, Vienna

Raskoff KA, Purcell JE, Hopcroft RR (2005) Gelatinous zooplankton of the Arctic Ocean: in situ observations under the ice. Polar Biol 28:207–217

Raskoff KA, Hopcroft RR, Kosobokova KN, Purcell JE, Youngbluth M (2010) Jellies under ice: ROV observations from the Arctic 2005 hidden ocean expedition. Deep Sea Res Part II 57:111–126

Robison BH (2004) Deep pelagic biology. J Exp Mar Biol Ecol 300:253–272

Roux JP, van der Lingen CD, Gibbons MJ, Moroff NE, Shannon LJ, Smith AD, Cury PM (2013) Jellyfication of marine ecosystems as a likely consequence of overfishing small pelagic fishes: lessons from the Benguela. Bull Mar Sci 89:249–284

Sakov P, Counillon F, Bertino L, Lisæter KA, Oke PR, Korablev A (2012) TOPAZ4: an ocean-sea ice data assimilation system for the North Atlantic and Arctic. Ocean Sci 8:633–656

Shiganova TA, Abyzova GA (2022) Revision of Beroidae (Ctenophora) in the southern seas of Europe: systematics and distribution based on genetics and morphology. Zool J Linn Soc 194:297–322

Skarðhamar J, Svendsen H (2010) Short-term hydrographic variability in a stratified Arctic fjord. Geol Soc Lond Spec Publ 344:51–60

Svendsen H, Beszczynska-Møller A, Hagen JO, Lefauconnier B, Tverberg V, Gerland S, Wiencke C (2002) The physical environment of Kongsfjorden–Krossfjorden, an Arctic fjord system in Svalbard. Polar Res 21:133–166

Svendsen H (1991) Preliminary results from a hydrophysical investigation of Porsangerfjord, Altafjord and adjacent coastal waters, June-August 1990. Report of the Geophysical Institute, University of Bergen, Norway

Swerpel S (1985) The Hornsund fjord: water masses. Pol Polar Res 475–496

Titelman J, Gandon L, Goarant A, Nilsen T (2007) Intraguild predatory interactions between the jellyfish Cyanea capillata and Aurelia aurita. Mar Biol 152:745–756

Toyokawa M, Toda T, Kikuchi T, Miyake H, Hashimoto J (2003) Direct observations of a dense occurrence of Bolinopsis infundibulum (Ctenophora) near the seafloor under the Oyashio and notes on their feeding behavior. Deep Sea Res Part I 50:809–813

von Appen WJ, Wekerle C, Hehemann L, Schourup-Kristensen V, Konrad C, Iversen MH (2018) Observations of a submesoscale cyclonic filament in the marginal ice zone. Geophys Res Lett 45:6141–6149

Wassmann P, Svendsen H, Keck A, Reigstad M (1996) Selected aspects of the physical oceanography and particle fluxes in fjords of northern Norway. J Mar Syst 8:53–71

Wickham H, Chang W, Wickham MH (2016) Package 'ggplot2'. Create elegant data visualisations using the grammar of graphics. Version 2:1-189